

Time-Dependent Changes in Lipid Metabolism in Mice with Methionine Choline Deficiency-Induced Fatty Liver Disease

Han-Sol Park^{1,4}, Byeong Hwan Jeon^{1,4}, Sung Hoon Woo¹, Jaechan Leem², Jung Eun Jang²,
Min Sock Cho³, In-Sun Park³, Ki-Up Lee², and Eun Hee Koh^{2,*}

Methionine and choline-deficient diet (MCD)-induced fatty liver is one of the best-studied animal models of fatty liver disease. The present study was performed to clarify the relative contributions of individual lipid metabolic pathways to the pathogenesis of MCD-induced fatty liver. Hepatic lipogenesis mediated by the sterol regulatory element-binding protein (SREBP-1c) was increased at 1 week, but not at 6 weeks, of MCD feeding. On the other hand, ¹⁴C-palmitate oxidation did not change at 1 week, but significantly decreased at 6 weeks. This decrease was associated with increased expression of fatty acid translocase, a key enzyme involved in fatty acid uptake. Expression of endoplasmic reticulum stress markers was increased in mice given MCD for both 1 and 6 weeks. These findings suggest the presence of time-dependent differences in lipid metabolism in MCD-induced fatty liver disease: SREBP-1c-mediated lipogenesis is important in the early stages of fatty liver disease, whereas increased fatty acid uptake and decreased fatty acid oxidation become more important in the later stages.

INTRODUCTION

The increasing prevalence of obesity has led to a rapid increase in the incidence of non-alcoholic fatty liver disease (NAFLD) in industrialized countries (Schattenberg and Galle, 2010). Its progressive form, non-alcoholic steatohepatitis (NASH), can lead to cirrhosis and end-stage liver disease (Larter and Yeh, 2008). The main risk factors for NAFLD are the metabolic abnormalities commonly observed in metabolic syndrome, including insulin resistance, visceral obesity and dyslipidemia. However, certain diets and toxins can also induce NAFLD (Koteish and Diehl, 2001). Methionine and choline-deficient diet (MCD)-induced fatty liver is one of the best-studied animal models of NAFLD (Mato et al., 2008). In particular, this model is important for understanding the mechanism of NAFLD progression, since long-term administration of MCD has been

shown to cause NASH, liver cirrhosis and hepatocellular carcinoma (Nakae, 1999).

Endoplasmic reticulum (ER) stress and sterol regulatory element-binding protein isoform-1c (SREBP-1c)-dependent lipogenesis are considered important in the pathogenesis of fatty liver disease (Kaplowitz and Ji, 2006; Sozio et al., 2010). Lipogenesis in the liver is transcriptionally regulated by SREBP-1c and carbohydrate-responsive element-binding protein, with SREBP-1c considered a major regulator of the lipogenic pathway (Ferré and Foufelle, 2010). The mature form of SREBP-1c is embedded in the membranes of the ER. In the presence of adequate signals (e.g., insulin, ER stress), SREBP-1c is activated by proteolytic cleavage and becomes involved in promoting lipid synthesis (Ferré and Foufelle, 2010).

However, studies in humans and in rodents have demonstrated that other pathways of lipid metabolism are also involved in the genesis of NAFLD. Excess fat accumulation in the liver can result from increased fatty acid delivery, from fat stored in white adipose tissue that flows to the liver by way of the plasma free fatty acid (FFA) pool; increased de novo fatty acid synthesis from glucose; reduced fatty acid oxidation; and/or reduced triglyceride (TG) export in the form of very low-density lipoprotein (VLDL) (Ferré and Foufelle, 2010; Postic and Girard, 2008). The roles of these different pathways of lipid metabolism and ER stress in MCD-induced fatty liver disease are not clear. MCD feeding has been shown to increase fatty acid uptake and to decrease VLDL secretion, as well as to downregulate genes involved in lipid synthesis (Rinella et al., 2008). Recent studies reported that MCD feeding significantly increases the expression of ER stress markers (Jr Soon et al., 2010; Mu et al., 2010), but another study proposed that this stress response alone does not lead to liver injury (Jr Soon et al., 2010).

We sought to clarify the roles of various pathways of lipid metabolism and ER stress in the pathogenesis of MCD-induced NAFLD. We found that SREBP-1c-induced lipogenesis is important in the early stages of fatty liver disease, whereas increased fatty acid uptake and decreased fatty acid oxidation

¹Asan Institute for Life Sciences, University of Ulsan College of Medicine, Seoul 138-736, Korea, ²Department of Internal Medicine, University of Ulsan College of Medicine, Seoul 138-736, Korea, ³Department of Anatomy, College of Medicine, Inha University, Incheon 401-103, Korea, ⁴These authors contributed equally to this work.

*Correspondence: ehk@amc.seoul.kr

Table 1. Composition of MCD

| Nutrient | MCD |
|-------------------------------------|-------|
| L-Amino acids | 142.0 |
| L-Methionine | 0.0 |
| Choline chloride | 0.0 |
| Cornstarch | 100.0 |
| Dextrin | 100.0 |
| Sucrose | 408.6 |
| Cellulose | 50.0 |
| Corn oil | 50.0 |
| Sodium bicarbonate | 4.3 |
| Primex (hydrogenated vegetable oil) | 100.0 |
| Salt mix | 35.0 |
| Vitamin mix | 10.0 |
| Ferric citrate | 0.1 |

become more important in the later stages of this disease.

MATERIALS AND METHODS

Animal experiments

Eight-week-old C57BL/6J mice were purchased from Central Animal Laboratory (Korea). All mice were housed at ambient temperature (22°C ± 1°C) with 12:12-h light:dark cycles and free access to water and diet. All animal experiments were approved by the Institutional Animal Care and Use Committee of the Asan Institute for Life Sciences. One group of mice (n = 7) was fed normal chow, whereas a second group of mice (n = 7) was fed MCD (no, 518810; Dyets, USA). The composition of MCD is shown in Table 1. After 1 and 6 weeks, the mice were fasted for 5 h in the morning and sacrificed. Their livers were rapidly removed and kept frozen at -70°C.

Analysis of blood samples

Plasma TG (Sigma, USA), cholesterol (BioVision, USA) and FFA concentrations (Wako, Japan) were measured by enzymatic methods according to the manufacturers' instructions. Serum alanine aminotransferase (ALT) concentrations were measured using an IDTox Alanine Transaminase Endpoint Assay Kit (ID Labs Inc., Canada).

Liver TG and cholesterol contents

TG and cholesterol contents in the liver were determined using GPO-Trinder (Sigma) and cholesterol quantification (BioVision) kits, respectively, as described by their manufacturers.

Histological analysis

Liver tissue samples were fixed with 4% paraformaldehyde, embedded in paraffin, and stained with hematoxylin and eosin (H&E). Hepatic fibrosis was analyzed by trichrome C staining. Images were captured using a BX60 camera (Olympus, Japan). For measurements of lipid droplet size, 25 lipid droplets were randomly selected from four different sections of liver tissue for each mouse. For fibrotic area measurements, four random fields from each sample were selected. Quantification of lipid droplet size and fibrotic area was carried out using NIH Image J software (version 1.42q). Data are expressed as percentage of total sectional area, with each area represented as fold-increase relative to that in age-matched control mice.

Table 2. Gene-specific primers for real-time PCR

| mRNA | Primer sequence |
|----------|--------------------------------|
| SREBP-1c | 5'-CTGGGGGTGAGACAGGGGAC-3' |
| | 5'-GATGGTGGAGGGGACAAGGG-3' |
| FAS | 5'-CTGAGCGGCTCTGTTCCTT-3' |
| | 5'-CCCAGCTATGCGGTAGGGTC-3' |
| Insig2a | 5'-CCCTCAATGAATGTAAGGATT-3' |
| | 5'-TGTGAAGTGAAGCAGACCAATGT-3' |
| GPAT1 | 5'-TCGACCTAGGCTTCTCCGGG-3' |
| | 5'-GACGGGACAGTTGTGCTGGG-3' |
| DGAT2 | 5'-GATCGCAGTGGGTGCGAAAC-3' |
| | 5'-ATGCCATGGGGGTGGTATCC-3' |
| XBP-1s | 5'-ACACGCTTGGGAATGGACAC-3' |
| | 5'-CCATGGGAAGATGTTCTGGG-3' |
| ACO | 5'-TGTTAAGAAGAGTGCCACCAT-3' |
| | 5'-ATCCATCTCTTCATAACCAAATTT-3' |
| CPT1 | 5'-ACTCCTGGAAGAAGAAGTTCA-3' |
| | 5'-AGTATCTTTGACAGCTGGGAC-3' |
| MCAD | 5'-CACCGCAGCTTCCGGAATGT-3' |
| | 5'-TCGAAAGCGGCTCACAAAGCAG-3' |
| FAT/CD36 | 5'-AATTAGTAGAACCGGGCCAC-3' |
| | 5'-CCAACCTCCAGGTACAATCA-3' |

Fatty acid oxidation

Fatty acid oxidation (FAO) rate was measured as ¹⁴C₂ generation from [¹⁴C] palmitate (NEN Life Sciences, USA), as previously described (Kim et al., 2002), with minor modifications. Briefly, 50 μl of liver homogenate was added to a reaction mixture containing 0.2 mM palmitate (1-¹⁴C palmitate at 0.5 μCi/ml) and incubated for 30 min. at 30°C. Reactions were stopped by adding 50 μl of 4 N sulfuric acid, and the CO₂ produced was trapped with 200 μl of 1N sodium hydroxide. The trapped ¹⁴CO₂ and the ¹⁴C-labeled acid soluble products were measured by liquid scintillation counting, and FAO rates were normalized to the protein content of each tissue sample.

Western blot analysis

Protein expression in cells and tissues was measured by Western blot analysis. Isolated liver samples were lysed, loaded (30 μg per lane) onto 10% SDS-polyacrylamide gels, electrophoresed, and transferred to nitrocellulose membranes. After incubating in blocking buffer, the membranes were incubated with antibodies to (phospho) eukaryotic translation initiation factor 2α (eIF2α; Cell Signaling Technology, USA), CCAAT/enhancer-binding protein (CHOP; Santa Cruz Biotechnology, USA) and β-actin (Sigma), washed and then incubated with horseradish peroxidase-conjugated secondary antibodies (Santa Cruz Biotechnology). Immunoreactive bands were visualized by enhanced chemiluminescence (Santa Cruz Biotechnology) and quantified densitometrically. Results were normalized to β-actin to correct for variations in sample loading and are expressed as percentages of control signals (% control) in each blot to correct for variations between blots.

Quantification of mRNA levels

Total RNA was isolated using the TRIzol reagent (Invitrogen, USA), and 1-μg aliquots were reverse-transcribed with random primers using a Reverse Aid M-MuLV reverse transcription kit

Table 3. Metabolic parameters of mice fed MCD

| | 1 week | | 6 weeks | |
|---------------------------------|--------------|---------------|--------------|--------------|
| | CON | MCD | CON | MCD |
| Body weight (g) | 22.5 ± 0.3 | 19.6 ± 0.2* | 26.5 ± 0.3 | 15.7 ± 0.8* |
| Liver weight (g) | 1.1 ± 0.1 | 0.8 ± 0.1* | 1.1 ± 0.1 | 0.7 ± 0.1* |
| Liver TG (mg/g tissue) | 26.9 ± 2.5 | 69.6 ± 5.5* | 29.5 ± 5.2 | 98.2 ± 11.5* |
| Liver cholesterol (μg/g tissue) | 1.2 ± 0.1 | 3.6 ± 0.3* | 3.3 ± 0.4 | 2.6 ± 0.1 |
| Plasma TG (mg/dl) | 156.4 ± 11.5 | 103.9 ± 8.8* | 168.9 ± 15.0 | 116.2 ± 9.7* |
| Plasma FFA (μEq/L) | 891.0 ± 56.3 | 550.0 ± 54.2* | 635.9 ± 90.7 | 520.5 ± 40.9 |

Values are means ± SEMs (n = 7 each).

**P* < 0.05 compared with control mice.

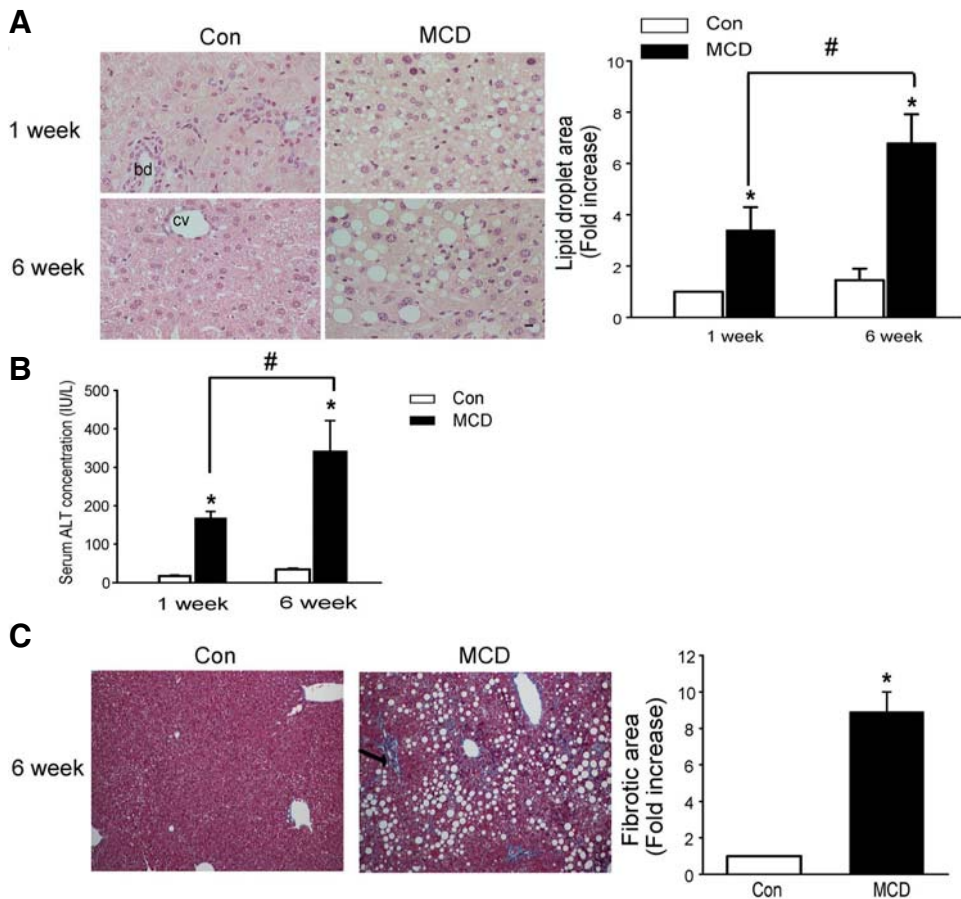


Fig. 1. MCD induces fatty liver disease. (A) Histological analysis of liver sections of MCD-fed mice. H&E staining. bd, bile duct; cv, central vein. The percentage of the total area of liver sections occupied by lipid droplets was quantified using an image analysis system. (B) Serum ALT concentrations in MCD-fed and control mice. (C) Trichrome C staining of mice given MCD for 6 weeks and control mice. The arrow (blue) indicates the accumulation of collagen fibers. Magnification, ×100. The percentage of fibrotic area was quantified using an image analysis system, and is represented as fold-increase relative to that in control mice. Data are means ± SEMs (n = 7 each). **P* < 0.05 versus age-matched control mice; #*P* < 0.05 versus mice given MCD for 1 week.

(Fermentas, USA). Target cDNA levels were quantified by SYBR green-based real-time polymerase chain reaction (PCR) using gene-specific primers (Table 2) and the ABI PRISM 7000 sequence detection system (Applied Biosystems, USA), as described previously (Won et al., 2010).

Statistical analysis

All results are reported as means ± standard errors of the mean (SEMs). Between-group differences were assessed using unpaired two-tailed *t*-tests. *P*-values < 0.05 were considered statistically significant. All data were analyzed using the SPSS program (version 17.0).

RESULTS

MCD feeding induces lipid accumulation and fibrosis in the liver

In agreement with previous results (Rinella et al., 2008), feeding of MCD for 1 and 6 weeks led to significant reductions in body weight and liver weight (Table 3). However, H&E staining showed that MCD significantly increased hepatic lipid accumulation (Fig. 1A). Hepatic levels of TG and cholesterol were also increased in MCD-fed mice (Table 3). Moreover, serum ALT levels were significantly higher in mice fed MCD for 1 week than in control mice, a difference that became more pronounced in mice fed MCD for 6 weeks (Fig. 1B). Trichrome C

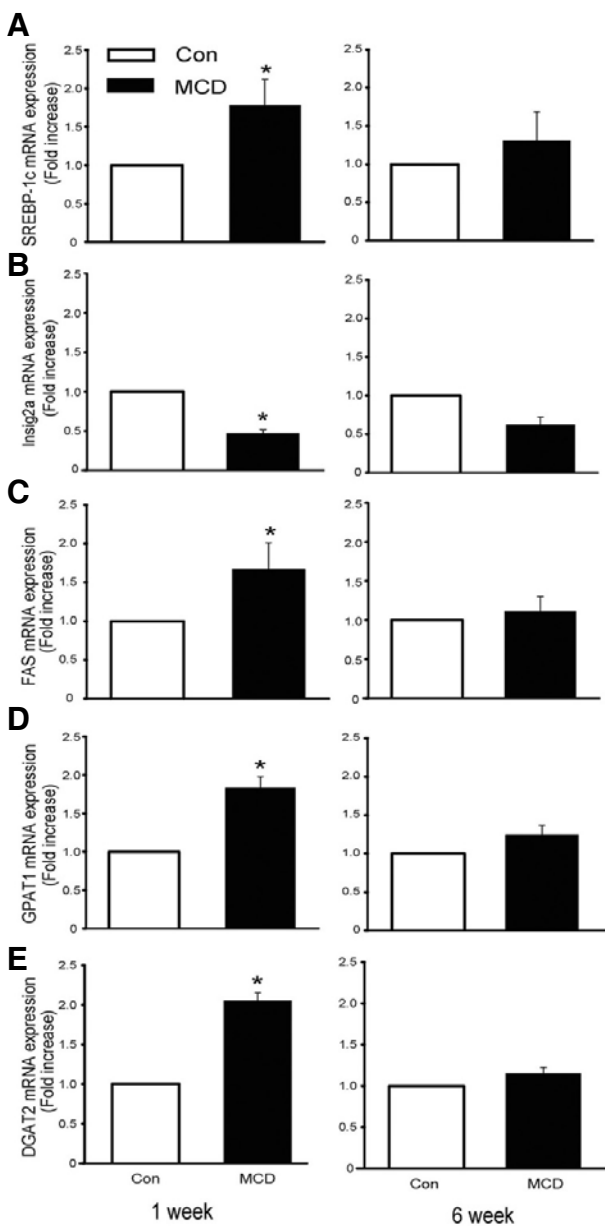


Fig. 2. MCD feeding for 1 week increases mRNA expression of de novo lipogenesis genes. Real-time PCR analysis of the expression of mRNAs encoding (A) SREBP-1c, (B) Insig2a, (C) FAS, (D) GPAT1 and (E) DGAT2. Values are means \pm SEMs ($n = 7$ each). * $P < 0.05$ versus control mice.

staining showed that MCD feeding for 6 weeks increased hepatic fibrosis (Fig. 1C).

Expression of lipogenic genes is increased after 1 week of MCD feeding

To examine the biochemical mechanisms underlying MCD-induced fatty liver disease, we first analyzed the expression levels of mRNA encoding molecules involved in de novo lipid synthesis from glucose (Postic and Girard, 2008). We found that the mRNA levels of SREBP-1c and the lipogenic genes fatty acid synthase (FAS), glycerol-3-phosphate acyltransferase 1 (GPAT1) and diacylglycerol transferase 2 (DGAT2) were all

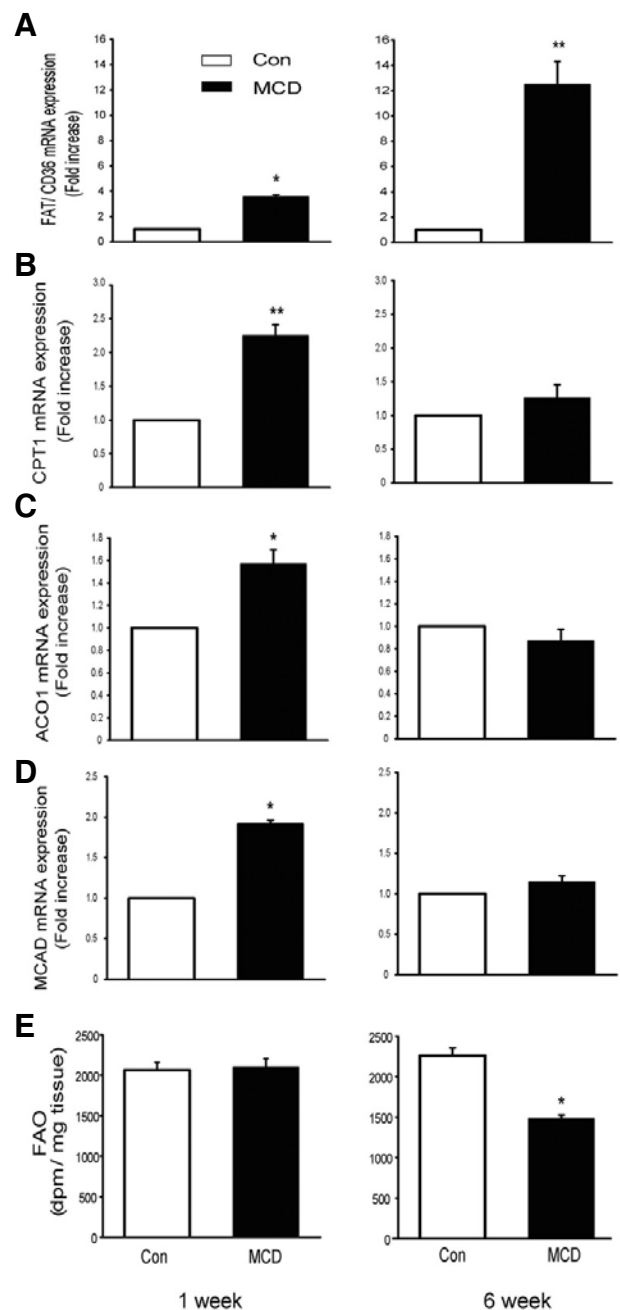


Fig. 3. MCD feeding for 6 weeks increases fatty acid uptake and decreases FAO. (A) Increased expression of FAT/CD36 mRNA. (B-D) Increased expression of mRNAs encoding FAO genes at 1 week, but not at 6 weeks, of MCD feeding. (B) CPT1, (C) ACO1, (D) MCAD. (E) Decreased ^{14}C -palmitate oxidation at 6 weeks of MCD feeding. Values are means \pm SEMs ($n = 7$ each). * $P < 0.05$, ** $P < 0.01$ versus control mice.

significantly increased in mice fed MCD for 1 week, and the mRNA level of Insig2a, which has been shown to inhibit SREBP-1c transport to the Golgi (Yabe et al., 2002), was significantly decreased (Fig. 2). In contrast, this increase in the expression of the lipogenic genes was not observed after 6 weeks of MCD feeding (Fig. 2).

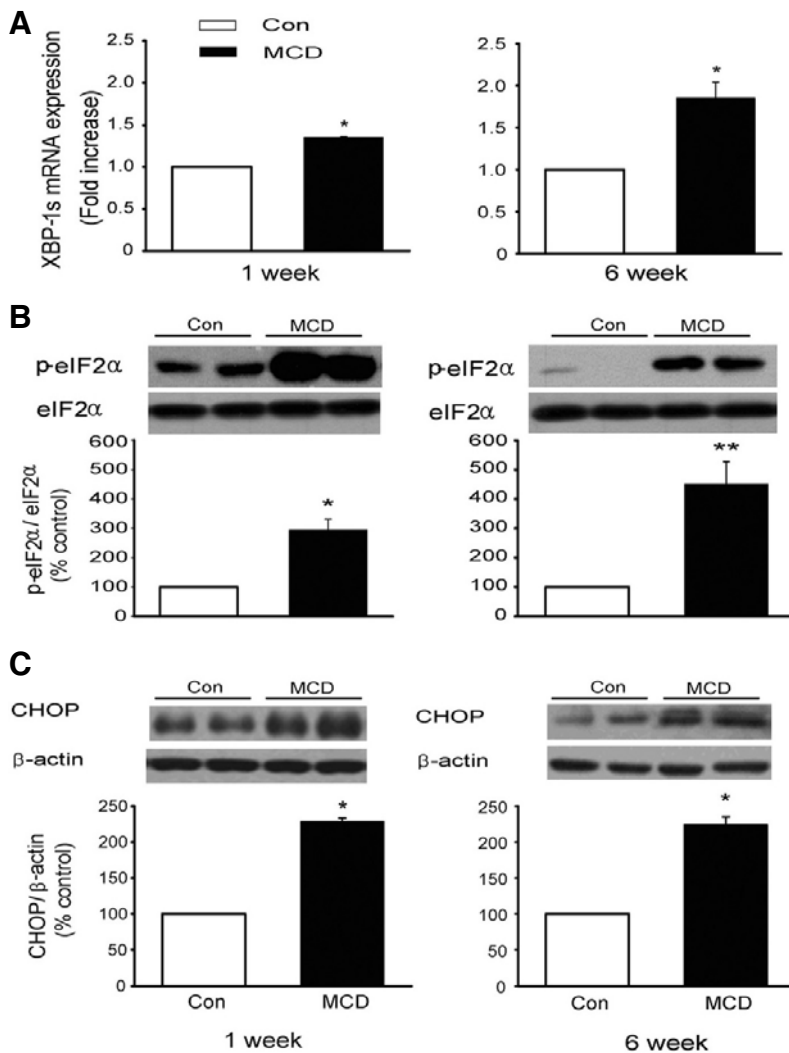


Fig. 4. Effect of MCD feeding on the ER stress response. (A) Real-time PCR analysis of spliced XBP-1s mRNA expression; (B, C) Western blot analysis of (B) eIF2 α phosphorylation and (C) CHOP protein expression. Protein levels were normalized to the expression of (B) total eIF2 α and (C) β -actin. Values are means \pm SEMs (n = 7 each). * P < 0.05, ** P < 0.01 versus control mice.

MCD feeding for 6 weeks increases fatty acid translocase expression and decreases FAO

Another source of fatty acids for hepatic TG is plasma FFA arising from adipose tissue. Increased FFA delivery, reduced FAO and/or reduced TG export in the form of VLDL would result in steatosis (Ferré and Foufelle, 2010; Postic and Girard, 2008). As expected from their lower body weights, plasma FFA concentrations were significantly lower in mice fed MCD for 1 week than in control mice (Table 3). However, the expression level of mRNA encoding fatty acid translocase (FAT)/CD36, the key enzyme involved in fatty acid uptake, was significantly increased in mice fed MCD for 1 week. Similarly, the expression levels of mRNAs encoding the FAO genes, carnitine palmitoyl-transferase 1 (CPT1), acyl-CoA oxidase 1 (ACO1) and medium chain acyl CoA dehydrogenase (MCAD), were significantly higher in mice fed MCD for 1 week than in control mice (Figs. 3A-3D). However, FAO measured by ^{14}C -palmitate was similar in mice fed MCD for 1 week and control mice (Fig. 3E), suggesting that increased mRNA expression of the genes responsible for fatty acid uptake and FAO in MCD-fed mice serves to compensate for the decrease in fatty acid delivery from plasma.

Plasma FFA concentration also tended to be lower in mice fed MCD for 6 weeks than in control mice, but the difference

was not statistically significant (Table 3). FAT/CD36 mRNA expression was markedly increased in mice fed MCD, whereas the expression of FAO genes did not differ significantly from that in control mice. However, FAO measured by ^{14}C -palmitate was significantly lower in mice fed MCD for 6 weeks than in control mice (Fig. 3E). Plasma TG concentration was significantly lower in mice fed MCD for 1 and 6 weeks than in control mice (Table 3).

MCD activates the ER stress response

Various markers for the ER stress response, namely mRNA expression of spliced X box-binding protein 1 (XBP-1s), phosphorylation of eIF2 α protein, and the expression of CHOP protein, were increased in mice fed MCD for both 1 and 6 weeks (Fig. 4).

DISCUSSION

The MCD diet results in liver injury that is similar to human NASH. A previous study has shown that MCD feeding for 4 weeks upregulates hepatic fatty acid transport proteins and increases hepatic uptake of ^{14}C -linoleic acid (Rinella et al., 2008). We also observed that the expression of FAT/CD36

profoundly increased in mice fed MCD for 6 weeks. In addition, we found time-dependent differences in lipid metabolism in MCD-induced NAFLD. The expression of SREBP-1c and lipogenic enzymes was significantly increased in mice fed MCD for 1 week, but this increase was not observed in mice fed MCD for 6 weeks. In contrast, MCD feeding for 6 weeks significantly decreased FAO, measured with ^{14}C -palmitate, and also increased FAT/CD36 expression.

MCD feeding for 1 week significantly increased the mRNA expression levels of SREBP-1c and the lipogenic enzymes FAS, GPAT1 and DGAT2. This suggests that the SREBP1c-dependent increase in de novo lipogenesis is the main mechanism of early steatosis in MCD-fed mice. It has been estimated that ~60% of hepatic TGs in obese humans are derived from the increased availability of plasma FFA, which is generated by unabated lipolysis of the larger adipose tissue mass (Donnelly et al., 2005; Ferré and Foufelle, 2010). On the other hand, MCD feeding led to significant weight loss and a significant reduction in plasma FFA concentration. Therefore, increased delivery of plasma FFA may not be the major mechanism for hepatic steatosis. In our study, mRNA expression levels of FAT/CD36, which is responsible for fatty acid uptake, and the enzymes responsible for FAO, were increased at 1 week of MCD feeding. However, FAO measured by ^{14}C -palmitate was similar in MCD-fed mice and control mice. Taken together with the reduced plasma FFA level in these mice, these results suggest that increased expression of enzymes responsible for fatty acid uptake and oxidation in the liver serve to compensate for the decrease in FFA delivery from plasma.

MCD feeding for 4 weeks has been shown to increase hepatic fatty acid uptake and to decrease VLDL secretion from the liver (Rinella et al., 2008). In agreement, we found that plasma TG concentration, a measure of VLDL export, was significantly decreased in mice fed MCD for 6 weeks. While the plasma FFA level was not significantly different from that in control mice, the expression of FAT/CD36 in the liver was profoundly increased, suggesting an increase in hepatic FFA uptake. In addition, measurement of FAO by ^{14}C -palmitate showed that MCD feeding for 6 weeks clearly decreased FAO in the liver, although the expression of FAO genes in these mice did not differ significantly from that in control mice. Oversupply of fatty acid, when not coupled with mitochondrial oxidation, can lead to increased biosynthesis of sphingolipids, including ceramide (Dara et al., 2011). The synthesis of sphingomyelin from ceramide and phosphatidylcholine also generates diacylglycerol (Dara et al., 2011). Ceramide and diacylglycerol, which were recently shown to be important mediators of inflammation and cell death (Coward 2009; Kennedy et al., 2009; Won et al., 2010), may mediate progression to NASH. Further studies, including measurement of these lipid metabolites, are needed to answer this important question.

The ER is responsible for the folding and assembly of membrane and secreted proteins, the synthesis of lipids and sterols, and the storage of calcium (Kaufman, 2002). The accumulation of misfolded or unfolded proteins in the ER lumen can activate a group of signal transduction pathways collectively termed the ER stress response or the unfolded protein response. In animal models of obesity and type 2 diabetes, ER stress has been shown to upregulate the lipogenic transcription factor SREBP-1c and lipogenic genes, resulting in hepatic steatosis (Kaufman, 2002; Tabas and Ron, 2011).

Although these data suggest that ER stress-mediated lipogenesis is an important mechanism of hepatic steatosis, it remains unclear whether the ER stress response is detrimental and contributes to progression to NASH or hepatic fibrosis (Ji,

2008). Deficiencies in CHOP, a key component of ER stress-mediated apoptosis, have been shown to attenuate liver fibrosis by reducing hepatocyte injury in bile duct-ligated mice (Tamaki et al., 2008). MCD was also shown to induce ER stress and hepatic cell death through activation of protein kinase C- δ (Greene et al., 2010). In contrast, a recent study suggested that the ER stress response itself does not lead to liver injury, and that CHOP does not play a central role in the pathogenesis of MCD-mediated liver disease (Jr Soon et al., 2010). We found that MCD feeding for both 1 and 6 weeks led to a significant increase in ER stress-response markers, whereas SREBP1c expression was increased only at 1 week, but not at 6 weeks, of MCD feeding. These results suggest that the ER stress response is not only involved in the early states of hepatic steatosis, but also in the later stages of progression to NASH (Greene et al., 2010; Tamaki et al., 2008). However, further studies are needed to determine the mechanism underlying the increased ER stress response and its meaning in the pathogenesis of steatosis and NASH in MCD-fed mice.

In summary, our results showed that increased de novo lipogenesis is an important determinant of early-stage fatty liver disease in MCD-fed mice, whereas increased fatty acid uptake and decreased FAO are major factors leading to later changes in fatty liver disease, including inflammation and fibrosis. MCD feeding for both 1 and 6 weeks led to a significant increase in ER stress-response markers. Future studies are needed to determine the contribution of ER stress to each stage (steatosis and inflammation) of the disease.

ACKNOWLEDGMENTS

This work was supported by the Korea Health Industry Development Institute (A084335).

REFERENCES

- Coward, L.A. (2009). Sphingolipids: players in the pathology of metabolic disease. *Trends Endocrinol. Metab.* 20, 34-42.
- Dara, L., Ji, C., and Kaplowitz, N. (2011). The contribution of endoplasmic reticulum stress to liver disease. *Hepatology* 53, 1752-1763.
- Donnelly, K.L., Smith, C.I., Schwarzenberg, S.J., Jessurun, J., Boldt, M.D., and Parks, E.J. (2005). Sources of fatty acids stored in liver and secreted via lipoproteins in patients with nonalcoholic fatty liver disease. *J. Clin. Invest.* 115, 1343-1351.
- Ferré, P., and Foufelle, F. (2010). Hepatic steatosis: a role for de novo lipogenesis and the transcription factor SREBP-1c. *Diabetes Obes. Metab.* 12, 83-92.
- Greene, M.W., Burrington, C.M., Ruhoff, M.S., Johnson, A.K., Chongkraitanakul, T., and Kangwanpomsiri, A. (2010). PKC δ is activated in a dietary model of steatohepatitis and regulates endoplasmic reticulum stress and cell death. *J. Biol. Chem.* 285, 42115-42129.
- Ji, C. (2008). Dissection of endoplasmic reticulum stress signaling in alcoholic and non-alcoholic liver injury. *J. Gastroenterol. Hepatol.* 23, S16-S24.
- Jr Soon, R.K., Yan, J.S., Grenert, J.P., and Maher, J.J. (2010). Stress signaling in the methionine-choline-deficient model of murine fatty liver disease. *Gastroenterology* 139, 1730-1739.
- Kaplowitz, N., and Ji, C. (2006). Unfolding new mechanisms of alcoholic liver disease in the endoplasmic reticulum. *J. Gastroenterol. Hepatol.* 21, S7-S9.
- Kaufman, R.J. (2002). Orchestrating the unfolded protein response in health and disease. *J. Clin. Invest.* 110, 1389-1398.
- Kennedy, A., Martinez, K., Chuang, C.C., LaPoint, K., and McIntosh, M. (2009). Saturated fatty acid-mediated inflammation and insulin resistance in adipose tissue: mechanisms of action and implications. *J. Nutr.* 139, 1-4.
- Kim, J.Y., Koves, T.R., Yu, G.S., Gulick, T., Cortright, R.N., Dohm, G.L., and Muoio, D.M. (2002). Evidence of a malonyl-CoA-insensitive carnitine palmitoyltransferase I activity in red skeletal

- muscle. *Am. J. Physiol. Endocrinol. Metab.* **282**, E1014-E1022.
- Koteish, A., and Diehl, A.M. (2001). Animal models of steatosis. *Semin. Liver Dis.* **21**, 89-104.
- Larter, C.Z., and Yeh, M.M. (2008). Animal models of NASH: getting both pathology and metabolic context right. *J. Gastroenterol. Hepatol.* **23**, 1635-1648.
- Mato, J.M., Martínez-Chantar, M.L., and Lu, S.C. (2008). Methionine metabolism and liver disease. *Annu. Rev. Nutr.* **28**, 273-293.
- Mu, Y.P., Ogawa, T., and Kawada, N. (2010). Reversibility of fibrosis, inflammation, and endoplasmic reticulum stress in the liver of rats fed a methionine-choline-deficient diet. *Lab. Invest.* **90**, 245-256.
- Nakae, D. (1999). Endogenous liver carcinogenesis in the rat. *Pathol. Int.* **49**, 1028-1042.
- Postic, C., and Girard, J. (2008). Contribution of de novo fatty acid synthesis to hepatic steatosis and insulin resistance: lessons from genetically engineered mice. *J. Clin. Invest.* **118**, 829-838.
- Rinella, M.E., Elias, M.S., Smolak, R.R., Fu, T., Borensztajn, J., and Green, R.M. (2008). Mechanisms of hepatic steatosis in mice fed a lipogenic methionine choline-deficient diet. *J. Lipid Res.* **49**, 1068-1076.
- Schattenberg, J.M., and Galle, P.R. (2010). Animal models of non-alcoholic steatohepatitis: of mice and man. *Dig. Dis.* **28**, 247-254.
- Sozio, M.S., Liangpunsakul, S., and Crabb, D. (2010). The role of lipid metabolism in the pathogenesis of alcoholic and non-alcoholic hepatic steatosis. *Semin. Liver Dis.* **30**, 378-390.
- Tabas, I., and Ron, D. (2011). Integrating the mechanisms of apoptosis induced by endoplasmic reticulum stress. *Nat. Cell Biol.* **13**, 184-190.
- Tamaki, N., Hatano, E., Taura, K., Tada, M., Kodama, Y., Nitta, T., Iwaisako, K., Seo, S., Nakajima, A., Ikai, I., et al. (2008). CHOP deficiency attenuates cholestasis-induced liver fibrosis by reduction of hepatocyte injury. *Am. J. Physiol. Gastrointest. Liver Physiol.* **294**, G498-G505.
- Won, J.C., Park, J.Y., Kim, Y.M., Koh, E.H., Seol, S., Jeon, B.H., Han, J., Kim, J.R., Park, T.S., Choi, C.S., et al. (2010). Peroxisome proliferator-activated receptor-gamma coactivator 1-alpha overexpression prevents endothelial apoptosis by increasing ATP/ADP translocase activity. *Arterioscler. Thromb. Vasc. Biol.* **30**, 290-297.
- Yabe, D., Brown, M.S., and Goldstein, J.L. (2002). Insig-2, a second endoplasmic reticulum protein that binds SCAP and blocks export of sterol regulatory element-binding proteins. *Proc. Natl. Acad. Sci. USA* **99**, 12753-12758.